

Adaptation of Two Types of Processing Gains for UWB-IR Wireless Sensor Networks

İsmail Güvenç¹, *Member, IEEE*, Hüseyin Arslan², *Senior Member, IEEE*, Sinan Gezici³, *Member, IEEE*,
Hisashi Kobayashi⁴, *Life Fellow, IEEE*

Abstract

Ultrawideband impulse radio (UWB-IR) systems offer two kinds of processing gains that can be adaptively changed based on the interference level in the system so that quality of service (QoS) requirements are fulfilled. In this paper, an adaptive assignment scheme for two types of multiple access parameters in cluster based wireless sensor networks is investigated. A mathematical framework is developed for asynchronous communications using a Gaussian approximation method to model the multiple access interference in two cases: one with *fixed frame duration*, where the goal is to increase the average throughput, and the other with *fixed symbol duration*, where the goal is to increase the network lifetime. Extension of the analysis to multipath channels is carried out, and the validity of the Gaussian approximation is investigated using the Kullback-Leibler distance.

I. INTRODUCTION

Ultrawideband impulse radio (UWB-IR) is a highly promising physical layer technology for wireless sensor networks (WSNs) due to its unique characteristics such as low power transmission, low cost and low complexity transceiver circuitry, flexibility to transmit within a large unlicensed spectrum (as long as complying with regulatory power requirements), precise location capability, and secure transmission due to employed multiple access sequences. In a UWB-IR system, time-hopping (TH) codes are employed as a multiple access method [1]. By appropriately designing the TH codes, it is possible to control multiple access interference in UWB systems to a certain extent [2], [3]. The TH multiple access can provide interference free communications in synchronous systems. Even in an asynchronous system, excessive interference can be avoided due to low duty cycle and large processing gain of UWB-IR pulse transmission.

Adaptation of wireless communication systems allows better exploitation of the system resources based on the estimation of wireless link quality [4]. The link quality is often measured by the signal-to-interference plus noise ratio (SINR) of the received signal. For example, adaptive coding [5], [6] schemes can achieve higher throughput when the channel quality is good by decreasing the amount of redundancy transmitted (or, increasing the modulation

¹DoCoMo USA Labs, 3240 Hillview Avenue, Palo Alto, CA 94304, USA, email: iguvenç@docomolabs-usa.com

²Electrical Engineering Dept., Univ. of South Florida, 4202 E. Fowler Ave., ENB-118, Tampa, FL 33620, USA, email: arslan@eng.usf.edu

³Department of Electrical and Electronics Engineering Bilkent University, Bilkent, Ankara 06800, email: gezici@ee.bilkent.edu.tr

⁴Department of Electrical Engineering, Princeton University, Princeton, NJ 08544, USA, email: hisashi@princeton.edu

order). On the other hand, when the link quality is poor, reliable transmission can be insured by increasing the amount of redundancy and coding power (or, by decreasing the modulation order). Assigning multiple codes to the users, changing the pulse shape [7] and duration, and changing the transmitted pulse power [8] as in conventional schemes are other forms of adaptation in UWB systems to better exploit the system resources.

Adaptation of multiple access parameters in UWB-IR systems is another flexible means of exploiting system resources efficiently. Different from many other technologies such as direct-sequence code division multiple access (DS-SS) systems, UWB-IR offers two different types of processing gains: number of pulses per symbol, and the frame duration. Increasing the number of pulses per symbol increases the SINR, which can be considered as a power control approach in the time domain without changing pulse amplitudes. Increasing the frame duration (which is related with the cardinality of the code) again improves the SINR in a multiuser environment, as it becomes less likely that the pulses will be corrupted. By measuring the link quality (which depends on the channel, multiuser interference etc.), it is possible to improve the data rate by modifying these two different multi-access parameters, while satisfying a minimum BER requirement set by QoS requirements. Alternatively, if a certain data rate is required by the system, by adjusting these two processing gains, the transmission power can be reduced to improve the network lifetime, when the link quality is good.

Adaptive rate and power allocation has been well studied for CDMA systems in the past [9]-[12]. Optimal assignment of number of pulses per symbol and the frame duration for UWB systems in range limited and multiuser interference limited environments were analyzed in [13], where the Gaussian approximation is used to characterize the link quality and assess data rate gains for asynchronous communications. In [14], use of the standard Gaussian approximation (SGA) to capture the multiple access interference (MAI) in power unbalanced scenarios was investigated, and it was shown to be applicable to densely deployed networks. Another Gaussian approximation of MAI for chip synchronous and chip asynchronous scenarios was derived in [15] for a system with fixed number of pulses per symbol and fixed frame duration. Although adaptation of frame duration and number of pulses per symbol was analyzed in [16] in the context of medium access control (MAC) for UWB ad hoc networks, a mathematical framework for the MAI has not been developed. In [17] and [18], the radio resource allocation problem was analyzed as a theoretical constraint optimization problem for ad hoc networks, where the system throughput is maximized considering a UWB physical layer, traffic patterns, and system topology. Both reserved bandwidth (QoS) and dynamic bandwidth (best effort) scenarios are considered, and admission policies of new users to the system are presented.

In this paper, adaptation of multiple access parameters is investigated in asynchronous environments for cluster based WSNs. Multiuser interference is modelled by a Gaussian approximation approach for two communication scenarios: *fixed frame duration*, where the goal is to maximize the overall data rate, and *fixed symbol duration*, where the goal is to have an identical data rate for all the users, and improve the network lifetime. For the fixed symbol duration case, the required symbol energy to meet the BER requirement is calculated, and the number of pulses to transmit is evaluated; this implies joint assignment of both the number of pulses per symbol and the frame duration, as the symbol duration is constant. Extension of the analysis to multipath channels is performed

for both cases. Also, the validity of the Gaussian approximation for different parameters is evaluated using the Kullback-Leibler (KL) distance metric, and its effects on the BER is analyzed for different parameters and SINRs. Improvements in the data rate and power consumption for the adaptation schemes are demonstrated with computer simulations for fixed and mobile cluster head scenarios. The main contributions of the paper can be summarized as follows: 1) Derivation of an asymptotic closed form expression for the probability distribution of MAI in an UWB-IR system with various frame durations for different users, 2) Evaluation of the asymptotic study by a metric based approach for various processing gain parameters, and 3) A processing gain adaptation framework for UWB-IR wireless sensor networks based on the asymptotic analysis.

The paper is organized as follows. Section II gives the system model for the UWB signaling and the sensor network. Adaptation schemes for asynchronous communications systems are analyzed in Section III and extensions to multipath channels are provided in Section IV. The validity of Gaussian approximation is investigated in Section V which is followed by the simulation results in Section VI. Finally, some concluding remarks are made.

II. SYSTEM MODEL

A. UWB Signal Model

In this section, a generic UWB signal model is introduced, where a variable number of pulses per symbol, as well as variable frame durations are allowed for different users. The transmitted UWB signal from user k in an N_u user system is given by

$$s_k(t) = \sqrt{E_{tp}^{(k)}} \sum_{j=-\infty}^{\infty} a_j^{(k)} b_{\lfloor j/N_s^{(k)} \rfloor}^{(k)} \omega_{tx}(t - jT_f^{(k)} - c_j^{(k)}T_c), \quad (1)$$

where $T_f^{(k)}$ is the frame duration of user k , j is the frame index, T_c is the chip duration, ω_{tx} represents the transmitted UWB pulse with unit energy, and $E_{tp}^{(k)}$ is the transmitted pulse energy for user k . The number of frames/pulses per information bit for user k is denoted as $N_s^{(k)} = T_s^{(k)}/T_f^{(k)}$, where $T_s^{(k)}$ is the symbol period for user k , and number of chips per frame of user k is denoted by $N_h^{(k)}$. The random polarity codes $a_j^{(k)}$ are binary random variables taking values ± 1 with equal probability, and $a_j^{(k)}$ and $a_i^{(l)}$ are independent for $(k, j) \neq (l, i)$ [19]. Also, $c_j^{(k)} \in \{0, 1, \dots, N_h^{(k)} - 1\}$ with equal probability, and $c_j^{(k)}$ and $c_i^{(l)}$ are independent for $(k, j) \neq (l, i)$. The transmitted bits of user k are denoted by $b_{\lfloor j/N_s^{(k)} \rfloor}^{(k)} \in \{-1, +1\}$.

The received signal over an AWGN channel is given by

$$r(t) = \sum_{k=1}^{N_u} \sqrt{E_{rp}^{(k)}} \sum_{j=-\infty}^{\infty} a_j^{(k)} b_{\lfloor j/N_s^{(k)} \rfloor}^{(k)} \omega_{rx}(t - jT_f^{(k)} - c_j^{(k)}T_c - \tau_k) + \sigma_n n(t), \quad (2)$$

where $E_{rp}^{(k)}$ is the received pulse energy, τ_k is the delay of user k , ω_{rx} denotes the received UWB pulse, and $n(t)$ is a zero mean white Gaussian noise process with unit spectral density.

Consider a MF receiver, as shown in Fig. 1, with the following template signal for the zeroth bit of user ξ ($b_0^{(\xi)}$),

without loss of generality:

$$s_{temp}^{(\xi)}(t) = \frac{1}{\sqrt{N_s^{(\xi)}}} \sum_{j=0}^{N_s^{(\xi)}-1} a_j^{(\xi)} \omega_{rx}(t - jT_f^{(\xi)} - c_j^{(\xi)}T_c - \tau_\xi) . \quad (3)$$

Then, the output of the MF is given by

$$Y = b_0^{(\xi)} \sqrt{E_{rp}^{(\xi)} N_s^{(\xi)}} + M + N , \quad (4)$$

where $N \sim \mathcal{N}(0, \sigma_n^2)$ is the output noise and M is the total MAI, which is the sum of interference terms from the interfering users:

$$M = \sum_{k=1, k \neq \xi}^{N_u} M_k , \quad (5)$$

where M_k is the MAI from user k . The statistics of M will be analyzed in Section III.

B. Sensor Network Model and BER Evaluation

A cluster based WSN is considered, where the cluster head has more complex circuitry, and therefore higher processing capabilities compared to the sensor nodes¹. The communication happens in rounds as in [20], where, after each round, the cluster head may update the multiple access parameters. Consider a cluster of N_u sensors, with the k th node having a transmitted pulse energy of $E_{tp}^{(k)}$ to communicate with the cluster head, which transmits the information to a remote base station. The received pulse energy for user k at the cluster head is given by

$$E_{rp}^{(k)} = E_{tp}^{(k)} \frac{\alpha_k}{d_k^n} , \quad (6)$$

where n denotes the path loss exponent, d_k is the distance between the k th sensor node and the cluster head, and α_k is the fading coefficient for user k . When there is no MAI, the probability of error for user k which employs binary phase shift keying (BPSK) modulation is given by

$$P_b^{(k)} = Q\left(\sqrt{\text{SNR}_k}\right) = Q\left(\sqrt{\frac{N_s^{(k)} E_{rp}^{(k)}}{\sigma_n^2}}\right) , \quad (7)$$

where, energy per symbol (bit) of user k is given by $E_{rs}^{(k)} = N_s^{(k)} E_{rp}^{(k)}$, $Q(x)$ is given by $\frac{1}{2} \text{erfc}(\frac{x}{\sqrt{2}})$, and SNR denotes the signal-to-noise ratio (interference effects will be considered later). Conventional UWB networks use the same number of pulses per symbol, and the same frame duration for each user, ensuring reliable communications with the user that has the worst link quality. If the minimum BER required by the system is given by P_b , the

¹In general, the cluster-head may also be selected from one of the sensor nodes as in [20]. However, this may increase the overall complexity of the network since larger complexity of the cluster-head will be required for each individual sensor node. On the other hand, the adaptation scheme to be introduced can be applied to other sensor network architectures with centralized control.

processing gain assigned to each user is given by

$$N_s = \frac{[Q^{-1}(P_b)]^2 \sigma_n^2}{E_{rp}^{min}}. \quad (8)$$

where E_{rp}^{min} denotes the minimum received pulse energy, which is from the furthest away user in an ideal environment. The raw data rate for each user is then given by $\frac{1}{N_s N_h T_c}$.

In order to better exploit the system resources, it is possible to change the number of pulses ($N_s^{(k)}$), and number of chips per frame ($N_h^{(k)}$), for each user based on the channel quality, the distance of the user from the cluster head, the long and short term fading effects, and the interference level in the system. In [3], a synchronous scenario is investigated where the orthogonal construction of TH sequences allows interference-free communications, such as in the downlink. However, synchronous signaling is not very practical for WSNs in general, and hence we focus on the asynchronous scenario in here. In the next section, adaptation of $N_s^{(k)}$ and $N_h^{(k)}$ in asynchronous systems is analyzed under a BER constraint and for two different cases: fixed frame duration (to maximize the data rate), and fixed symbol duration (to maximize the network lifetime).

III. PARAMETER ADAPTATION FOR ASYNCHRONOUS COMMUNICATIONS

In order to calculate the BER of the desired user in the presence of multiple users with random time hopping codes, we employ a Gaussian approximation approach for large number of *pulses* per information symbol. This is similar to the Gaussian approximations employed in [15] and [19]. However, we derive a more generic expression, which is valid for variable numbers of frame sizes, and covers the results in [15] and [19] as a special case.

For analytical purposes, we approximate an asynchronous UWB system by a chip-synchronous system, where the misalignment between the symbols of the users are integer multiples of the chip interval T_c . Assuming without loss of generality that the delay of the desired user is zero ($\tau_\xi = 0$), we assume that $\tau_k = \Delta_k T_c$ for $k \neq \xi$, where $\Delta_k \in \{0, 1, \dots, N_h^{(k)} N_s^{(k)} - 1\}$ with equal probability. As studied in [15], the chip-synchronous assumption usually results in over-estimating the error probability in random TH UWB-IR systems, and hence the system design based on this approximation is usually on the safe side.

A. Case 1: Fixed Throughput (Variable Frame Duration)

Consider the case where a fixed throughput is to be assigned to all users. Hence, we consider a common symbol time and BER in this scenario. In other words, the total processing gain, defined by $N_c = N_s^{(k)} N_h^{(k)}$, is constant in this case (see Fig. 2b, where $(N_s^{(1)}, N_h^{(1)}) = (3, 4)$, $(N_s^{(2)}, N_h^{(2)}) = (4, 3)$, and $(N_s^{(3)}, N_h^{(3)}) = (6, 2)$). Therefore, the number of pulses per symbol and the frame duration can be changed as long as their multiplication is fixed. In this case, the following lemma is employed in order to approximate the MAI from user k :

Lemma 1: *In a chip-synchronous scenario, the distribution of the MAI from user k converges to the following Gaussian random variable*

$$M_k \sim \mathcal{N} \left(0, \frac{E_{rp}^{(k)}}{N_h^{(k)}} \right), \quad (9)$$

as $\min\{N_s^{(\xi)}, N_s^{(k)}\} \longrightarrow \infty$.

Proof: See Appendix A.

In other words, for large values of $N_s^{(\xi)}$ and $N_s^{(k)}$, the MAI from user k converges to a zero mean Gaussian random variable. Note that the expression in (9) reduces to the result in [15] for $N_h^{(k)} = N_h^{(\xi)} \forall k$.

From (9), the total MAI can be approximated as

$$M \sim \mathcal{N} \left(0, \sum_{k=1, k \neq \xi}^{N_u} \frac{E_{rp}^{(k)}}{N_h^{(k)}} \right). \quad (10)$$

Then, the SINR of the system can be obtained as

$$\text{SINR} = \frac{N_s^{(\xi)} E_{rp}^{(\xi)}}{\sigma_n^2 + \sum_{k=1, k \neq \xi}^{N_u} \frac{E_{rp}^{(k)}}{N_h^{(k)}}}, \quad (11)$$

which can be expressed as

$$\text{SINR} = \frac{E_{rs}^{(\xi)}}{\sigma_n^2 + \frac{1}{N_c} \sum_{k=1, k \neq \xi}^{N_u} E_{rs}^{(k)}}, \quad (12)$$

by the defining the received *symbol* energy of the k th user by $E_{rs}^{(k)} = N_s^{(k)} E_{rp}^{(k)}$ for $k = 1, \dots, N_u$.

When the same SINR value is assigned to all the users, they have the same BER, hence the same throughput, as they have the same symbol time. Hence, from (12), it is observed that the same received symbol energy can be used to achieve the same BER for all users. That common energy, denoted by E_{rs} , can be obtained from (12) as

$$E_{rs} = \frac{\sigma_n^2 \text{SINR}}{1 - \left(\frac{N_u - 1}{N_c} \right) \text{SINR}}. \quad (13)$$

In other words, for a desired SINR value, the required received symbol energy of the users can be calculated. Since the symbol energy is the multiplication of the number of pulses per symbol and the pulse energy, the received symbol energy can be expressed as

$$E_{rs} = E_{ts}^{(k)} \frac{\alpha_k}{d_k^n} = N_s^{(k)} E_{tp}^{(k)} \frac{\alpha_k}{d_k^n}. \quad (14)$$

Therefore, the users can use different numbers of pulses per symbol and/or different pulse energy depending on the channel state and their location. In a practical setting, the cluster head can calculate the SINR for each of the users and feedback them how to scale their symbol energy in order to achieve the desired SINR. Note that when a user is very far away from the cluster head or its channel is in a deep fade, the transmitted symbol energy needs to be increased considerably, which might violate the FCC's regulations [21]. Therefore, multi-hopping might be necessary in some cases.

The received signal energy in (14) implies that given the fading coefficient and distance of user k , the energy can be set by changing $N_s^{(k)}$ and/or $E_{tp}^{(k)}$. In other words, there is a flexibility in adjusting the symbol energy. Note that this is different from the reserved bandwidth (RB) case in [17], since $N_s^{(k)}$ and $N_h^{(k)}$ are both variable (their

multiplication is constant) in our case. In [17], the RB case assumes $N_s^{(k)}$ is fixed (implying that $N_h^{(k)}$ is fixed as the data rate is fixed), and therefore the adaptation is acquired by only scaling $E_{tp}^{(k)}$.

Even though there is a flexibility in adjusting the received power, there are a few issues to consider when setting the symbol energy. First, the FCC's implicit limitation on the peak-to-average signal ratio can restrict the use of very small $N_s^{(k)}$ values. Secondly, the inter-frame interference (IFI) can be an issue in a multipath environment when choosing the number of frames per symbol, where choosing larger frames reduces the effects of the IFI.

B. Case 2: Fixed Frame Duration

In this case, the frame durations of all the users are the same. Hence, N_h is common for all of them (see for example Fig. 2a, where $N_s^{(1)} = 4$, $N_s^{(2)} = 3$, $N_s^{(3)} = 2$, and $N_h^{(k)} = 3$ for all k).

The aim is to meet the BER requirement for all users in the system. In order to satisfy a certain BER threshold, the number of pulses per symbol is adapted in order to maximize the overall data rate of the system [13].

The Gaussian approximation approach in the previous case can directly be applied to the fixed frame duration case² in which $N_h^{(k)} = N_h \forall k$. Then, the MAI from user k can be approximated by the following Gaussian random variable, when the number of pulses per information symbol for user ξ , $N_s^{(\xi)}$, is large:

$$M_k \sim \mathcal{N} \left(0, \frac{E_{rp}^{(k)}}{N_h} \right), \quad (15)$$

where $E_{rp}^{(k)}$ is the energy of a received pulse from user k .

From (15), (4) and (5), the SINR of the system for user ξ can be expressed as

$$\text{SINR} \approx \frac{N_s^{(\xi)} E_{rp}^{(\xi)}}{\sigma_n^2 + \frac{1}{N_h} \sum_{\substack{k=1 \\ k \neq \xi}}^{N_u} E_{rp}^{(k)}}, \quad (16)$$

from which the value of $N_s^{(\xi)}$ is obtained as

$$N_s^{(\xi)} = \left\lceil \frac{\text{SINR}}{\frac{E_{rp}^{(\xi)}}{N_h}} \left(\sigma_n^2 + \frac{1}{N_h} \sum_{\substack{k=1 \\ k \neq \xi}}^{N_u} E_{rp}^{(k)} \right) \right\rceil. \quad (17)$$

In other words, by setting the value of $N_s^{(\xi)}$ according to (17), we transmit just enough number of pulses per symbol to meet the BER requirement. This is contrary to conventional systems, where the worst case parameters are used for all users, hence a lower overall data rate is obtained. Note that all the users transmit with the same power over a block, however, for a given transmit power, the bit rate will depend on the link quality.

IV. EXTENSIONS TO MULTIPATH CHANNELS

Due to extremely short duration pulses employed, it is likely to observe individual multipath components (although not very dispersive) even in low-power and very short-range communications in densely deployed sensor

²This special case is also investigated in [15].

networks. Longer-range communications may yield much severe and dispersive channel impulse responses, where the maximum excess delay of the channel may be on the order of hundreds of nanoseconds. Therefore, it becomes very crucial to consider the effects of multipath, since it can have significant effects on the performance. Consider transmission over frequency selective channels, where the channel for user k is modeled as

$$h^{(k)}(t) = \sum_{l=1}^L \alpha_l^{(k)} \delta(t - (l-1)T_c - \tau_k), \quad (18)$$

where $\alpha_l^{(k)}$ and τ_k are the fading coefficient of the l th path and the delay of user k , respectively, and L is the total number of received taps. Assume that $\tau_1 = 0$ and $\sum_{l=1}^L |\alpha_l^{(k)}|^2 = 1$, without loss of generality.

From (1) and (18), the received signal can be expressed as

$$r(t) = \sum_{k=1}^{N_u} \sqrt{E_{rp}^{(k)}} \sum_{j=-\infty}^{\infty} a_j^{(k)} b_{[j/N_f]}^{(k)} u^{(k)}(t - jT_f^{(k)} - c_j^{(k)}T_c - \tau_k) + \sigma_n n(t), \quad (19)$$

where

$$u^{(k)}(t) = \sum_{l=1}^L \alpha_l^{(k)} \omega_{rx}(t - (l-1)T_c). \quad (20)$$

Consider a RAKE receiver for the ξ th user, which has the following template signal for the 0th information bit:

$$s_{temp}^{(\xi)}(t) = \frac{1}{\sqrt{N_s^{(\xi)}}} \sum_{j=0}^{N_s^{(\xi)}-1} a_j^{(\xi)} v(t - jT_f^{(\xi)} - c_j^{(\xi)}T_c), \quad (21)$$

where

$$v(t) = \sum_{l=1}^L \beta_l \omega_{rx}(t - (l-1)T_c), \quad (22)$$

with $\beta = [\beta_1, \dots, \beta_L]$ being the RAKE combining weights.

As considered in [22], the template signal given by (21) and (22) can represent different multipath diversity combining schemes by appropriate choices of the weighting vector β .

From (19)-(22), the output of the Rake receiver can be expressed as follows:

$$Y = \int r(t) s_{temp}^{(\xi)}(t) dt = b_0^{(\xi)} \sqrt{N_s^{(\xi)} E_{rp}^{(\xi)}} \sum_{l=1}^L \alpha_l^{(\xi)} \beta_l + M + N, \quad (23)$$

where the first term is the desired signal part, M is the MAI from other users and N is the output noise, which is approximately distributed as $N \sim \mathcal{N}\left(0, \sigma_n^2 \sum_{l=1}^L \beta_l^2\right)$ for large $N_s^{(\xi)}$ [22]. Assume $N_h^{(\xi)} \gg (L-1)$ so that the IFI and the inter-symbol interference (ISI) are negligible [23].

The MAI term in (23) can be expressed as in (5); that is, as the sum of MAI terms from other users.

For the fixed throughput case, the following result can be obtained.

Lemma 2: *In a chip-synchronous scenario, the distribution of the MAI from user k converges to the following*

Gaussian random variable

$$M_k \sim \mathcal{N}\left(0, \frac{E_{rp}^{(k)}}{N_h^{(k)}} \left[\sum_{j=1}^L \left(\sum_{l=1}^j \beta_l \alpha_{l+L-j}^{(k)} \right)^2 + \sum_{j=1}^{L-1} \left(\sum_{l=1}^j \alpha_l^{(k)} \beta_{l+L-j} \right)^2 \right] \right), \quad (24)$$

as $\min\{N_s^{(\xi)}, N_s^{(k)}\} \rightarrow \infty$.

Proof: See Appendix B.

Note that the result reduces to the result in [22] for $N_h^{(k)} = N_h^{(\xi)} = N_h \forall k$. That special case can be used for the fixed frame duration case to obtain the asymptotic MAI distribution as

$$M_k \sim \mathcal{N}\left(0, \frac{E_{rp}^{(k)}}{N_h} \left[\sum_{j=1}^L \left(\sum_{l=1}^j \beta_l \alpha_{l+L-j}^{(k)} \right)^2 + \sum_{j=1}^{L-1} \left(\sum_{l=1}^j \alpha_l^{(k)} \beta_{l+L-j} \right)^2 \right] \right) \quad (25)$$

for large $N_s^{(\xi)}$.

From (24) and (25), it is observed that the MAI from an interfering user converges, as $N_s^{(\xi)}$ and $N_s^{(k)}$ go to infinity, to Gaussian random variables with zero mean, similar to the ones in (9) and (15), respectively, with the only difference being the scaling factors to the variance terms, which purely depend on the multipath channel of the interfering user and the finger assignment of the RAKE receiver. In other words, the same dependence on the received pulse energy and the processing gain parameters (N_s and N_h) is preserved as in the AWGN case.

V. VALIDITY OF GAUSSIAN APPROXIMATION

In the previous sections, Gaussian approximations were used to model the multiuser interference in an asynchronous environment. In this section, the dependence of the accuracy of Gaussian approximation on the two types of processing gains is analyzed using the KL distance [24]. Moreover, the accuracy of the Gaussian approximation is evaluated for different multiple access parameters and SNR values.

A. KL Distance Between the Approximate and Actual MAI Distributions

Consider the equations (9) and (15) for *case 1* and *case 2*, respectively, where the interference from a second user was approximated using a Gaussian distribution with its variance depending on the parameters $N_s^{(\xi)}$, $N_h^{(k)}$, and $E_{rp}^{(k)}$ ($N_h^{(k)}$ is constant for *case 2*). In order to see how well the approximation captures the actual interference probability density function (PDF), the theoretical Gaussian PDF and the MAI PDF obtained from simulations can be compared for different ranges of multiple access parameters. The KL distance (or relative entropy) is commonly used to characterize the similarity between two distributions. Let $f_{theo}^{N_s^{(\xi)}, N_h^{(k)}}$ denote the PDF of the interference corresponding to a set of parameters $N_s^{(\xi)}$, $N_h^{(k)}$; and let $f_{sim}^{N_s^{(\xi)}, N_h^{(k)}}$ denote the PDF of the interference generated using simulations and corresponding to the same set of parameters. Then, the KL distance between two distributions is given by

$$K\left(f_{theo}^{N_s^{(\xi)}, N_h^{(k)}} \parallel f_{sim}^{N_s^{(\xi)}, N_h^{(k)}}\right) = \sum_{i=-\infty}^{\infty} f_{theo}^{N_s^{(\xi)}, N_h^{(k)}}(i) \times \ln \frac{f_{theo}^{N_s^{(\xi)}, N_h^{(k)}}(i)}{f_{sim}^{N_s^{(\xi)}, N_h^{(k)}}(i)}. \quad (26)$$

The larger the KL distance, the less would be the similarity between the two PDFs. As the KL distance metric is not symmetric, the average of the two KL distances (i.e. $K(f_{theo}||f_{sim})$ and $K(f_{sim}||f_{theo})$) is used in this paper to evaluate the similarity between the two distributions.

Note that while the interference distribution lies between $(-\sqrt{E_{rp}^{(\xi)} N_s^{(\xi)}}, \sqrt{E_{rp}^{(\xi)} N_s^{(\xi)}})$, the support of the theoretical Gaussian distribution is $(-\infty, \infty)$. Analyzing (26) under this fact implies that KL distance may converge to infinity if not properly treated. Therefore, as an approximation, we truncate the theoretical Gaussian distribution to lie within the support of the interference distribution, and the area under the omitted tails of the Gaussian distribution are included as delta functions at the edges of the truncated Gaussian distribution.

In Fig. 3, simulation results for *case 2* are presented for various values of frame durations and processing gains. Two users with equal power levels are considered, and the KL distances are computed for different values of $N_s^{(\xi)}$ and $N_h^{(k)}$. It is observed that the MAI converges to a Gaussian distribution for larger values of $N_s^{(\xi)}$, and for smaller values of $N_h^{(k)}$ (2.10^7 bits are used in simulations). Similar simulations are repeated for *case 1*, where similar results are observed.

B. BER Performances Using the GA and the Actual MAI Distribution

Even though the KL distance characterizes the accuracy of Gaussian approximation for different set of parameters (relative to another set of parameters), how much this will affect the BER is also dependent on SNR. For example, if the noise variance is large, inaccuracy of the Gaussian approximation may not yield significant deviations from the actual BER. On the other hand, BER of the systems operating at high SNR environments may be very sensitive against inaccuracies in the Gaussian approximation.

In Fig. 4, the BER vs. SNR curves for *case 2* and for different multiple access parameters are presented, which are obtained using the simulations and the Gaussian approximation. It is observed that the larger values of N_s increases the accuracy of Gaussian approximation. It is also seen that as the SNR increases, the deviation between the BERs obtained using the Gaussian approximation and the simulations increases. The theoretical and simulation BER results for four users were also presented for comparison purposes, where it can be observed that Gaussian approximation provides a tighter bound.

VI. SIMULATION RESULTS

Computer simulations are performed to demonstrate the improvements in the data rate and reductions in power consumption. Only a *single cluster* of a WSN is considered in the simulations, and 100 sensor nodes are randomly distributed over a 25×25 meters field. The results can also be generalized for multiple clusters, where sensor nodes in each cluster communicate adaptively with the cluster head, and the cluster heads (which form another upper-level cluster within themselves) communicate adaptively with the sink. Corresponding to a BER of 10^{-4} for BPSK modulation, SNR = 8.39dB is targeted. The path loss exponent is taken to be $n = 2.4$, the pulse width is set to $T_c = 0.3ns$, and the chip synchronous case is considered in all scenarios. It is assumed that the transmitted pulse occupies the whole 7.5GHz of bandwidth in between 3.1GHz – 10.6GHz. Since the FCC mask allows a maximum

transmission power of -41dBm/MHz within this frequency range, the maximum transmit energy per second can be calculated to be 0.562mW . This is the maximum power that any sensor can transmit within the limits of FCC regulations, which might restrict the selection of optimum N_h and N_s even if SINR is appropriate.

Simulation results for asynchronous scenario of *case 1* are presented in Figs. 5 and 6, where the data rates are identical for all the users: $(N_c T_c)^{-1} = (10^4 \times 0.3 \times 10^{-9})^{-1} = 33\text{kbps}$, with $N_c = N_s \times N_h = 10^4$. For simulation purposes, continuous transmission of all the sensors and very low initial battery energy assignments (1mJ) for each node are assumed. The parameters are updated after each round of $300\mu\text{sec}$ to adapt to the Rayleigh fading channel and possibly changed distances, and the energy consumption in 5×10^4 rounds is analyzed. Simulation results indicate substantial gains in network lifetime when using adaptive assignment of processing gain (PG). Also, the effects of mobility of the cluster head (CH) is analyzed. This may be considered, for example, for rescue-robot applications where the robot acts as a cluster head to communicate with various sensors, and although the power consumption of the robot is not that crucial, we would like to maximize the network lifetime of the sensors. It is observed in Figs. 5 and 6 that if the cluster head randomly moves in the network, the network lifetime shortens seriously. On the other hand, the movement of the cluster head after each round to an optimal location (i.e., the expected value of the locations of the *alive* sensor nodes) slightly increases the network lifetime compared to the case when the cluster head is motionless and located at the center of the network. In Fig. 7, we also compare (averaged over 10^4 sensor realizations) the metric $T_{0.95} = T_{0.95}^{(adapt)} / T_{0.95}^{(fixed)}$ for different parameters, where $T_{0.95}^{(adapt)}$ and $T_{0.95}^{(fixed)}$ are the time durations where the total network energy falls to 95% of the initial network energy for adaptive PG and fixed PG cases, respectively. We observe that as the number of sensor nodes increases or the network dimensions decreases (i.e., the sensor intensity increases), the gains obtained from the adaptive PG approach diminishes. In particular, for the $15 \times 15\text{m}^2$ scenario, there is almost no gain. This implies that the proposed technique is less appropriate for short-range communications where the path-loss is less severe. Nevertheless, as implied by Fig. 5, adaptive PG approach will still have merit for longer observation windows.

VII. CONCLUSION

In this paper, adaptation of multiple access parameters in cluster based UWB-IR WSNs has been analyzed. A Gaussian approximation method has been employed to adapt the transmission powers and the processing gains of the sensors, and a mathematical framework has been developed for the analysis of MAI when the users employ different numbers of pulses per symbol and different frame durations. The main contribution of the paper is on the analysis of variable frame duration case, both in AWGN and in multipath channels. Also, the accuracy of the Gaussian approximation has been investigated and quantified using the KL distance based on the parameters (N_s, N_h) in a way not addressed in the literature before. It has been shown to be accurate for populated networks with large N_s , small N_h , and low SNR values. Simulation results outline the potential improvements in energy savings using the adaptive system design based on the two parameters.

Many of the analysis discussed in the paper can also be extended to other centralized sensor architectures (not necessarily cluster-based) that employ UWB signals, where a central node controls the assignment of TH codes to

the other nodes. On the other hand, the Gaussian approximation framework can be applied to any asynchronous network. The authors believe that the proposed adaptation scheme can be used for cognitive communications for extending the capabilities of future wireless networks.

REFERENCES

- [1] M. Z. Win and R. A. Scholtz, "Impulse radio: How it works," *IEEE Commun. Letters*, vol. 2, no. 2, pp. 36–38, Feb. 1998.
- [2] I. Guvenc and H. Arslan, "Design and performance analysis of time hopping sequences for UWB-IR systems," in *Proc. IEEE Wireless Commun. Networking Conf. (WCNC)*, vol. 2, Atlanta, GA, Mar. 2004, pp. 914–919.
- [3] I. Guvenc, H. Arslan, S. Gezici, and H. Kobayashi, "Adaptation of multiple access parameters in time hopping UWB cluster based wireless sensor networks," in *Proc. IEEE Mobile Ad-hoc and Sensor Systems Conf. (MASS)*, Ft. Lauderdale, FL, Oct. 2004, pp. 235–244.
- [4] H. Arslan, *Adaptation Techniques and the Enabling Parameter Estimation Algorithms for Wireless Communication Systems*. Book Chapter, Signal Processing Communications Handbook, CRC Press, 2004.
- [5] J. Y. L. Boudec, R. Merz, B. Radunovic, and J. Widmer, "A MAC protocol for UWB very low power mobile ad-hoc networks based on dynamic channel coding with interference mitigation," EPFL Technical Report ID: IC/2004/02, Lausanne, Switzerland, Tech. Rep., Jan. 2004.
- [6] G. Giancola, L. D. Nardis, M. G. D. Benedetto, and E. Dubuis, "Dynamic resource allocation in time varying ultra wideband channels," in *Proc. IEEE Int. Conf. Commun. (ICC)*, vol. 6, Paris, France, June 2004, pp. 3581–3585.
- [7] H. Zhang and R. Kohno, "Soft-spectrum adaptation in UWB impulse radio," in *Proc. IEEE Personal Indoor Mobile Radio Commun. (PIMRC)*, vol. 1, Beijing, China, Sep. 2003, pp. 289–293.
- [8] S. S. Kolenchery, J. K. Townsend, J. A. Freebersyser, and G. Bilbro, "Performance of local power control in peer-to-peer impulse radio networks with bursty traffic," in *Proc. IEEE Global Telecommun. Conf.*, vol. 2, Phoenix, AR, Nov. 1997, pp. 910–916.
- [9] S. J. Oh and K. M. Wasserman, "Adaptive resource allocation in power constrained cdma mobile networks," in *Proc. IEEE Wireless Commun. Networking Conf. (WCNC)*, vol. 1, New Orleans, LA, Sept. 1999, pp. 510–514.
- [10] D. Kim, "Rate-regulated power control for supporting flexible transmission in future CDMA mobile networks," *IEEE J. Select. Areas Commun.*, vol. 17, no. 5, pp. 968–977, May 1999.
- [11] L. C. Yun and D. G. Messerschmitt, "Variable quality of service in CDMA systems by statistical power control," in *Proc. IEEE Int. Conf. Commun.*, vol. 2, Seattle, WA, June 1995, pp. 713–719.
- [12] F. Berggren and S. L. Kim, "Energy-efficient control of rate and power in DS-CDMA systems," *IEEE Trans. Wireless Commun.*, vol. 3, no. 3, pp. 725–733, May 2004.
- [13] J. Diaz and Y. Bar-ness, "Adaptive transmission for UWB impulse radio communications," in *Proc. Conf. on Information Sciences Syst. (CISS)*, Baltimore, MD, Mar. 2003.
- [14] G. Giancola, L. D. Nardis, and M. G. D. Benedetto, "Multi user interference in power-unbalanced ultra wide band systems: Analysis and verification," in *Proc. IEEE Ultrawideband Syst. Technol. Conf. UWBST*, Reston, VA, Nov. 2003, pp. 325–329.
- [15] S. Gezici, H. Kobayashi, H. V. Poor, and A. F. Molisch, "Performance evaluation of impulse radio UWB systems with pulse-based polarity randomization in asynchronous multiuser environments," in *Proc. IEEE Wireless Commun. Networking Conf. (WCNC)*, Atlanta, GA, Mar. 2004.
- [16] H. Yomo, P. Popovski, C. Wijting, I. Z. Kovacs, N. Deblauwe, A. F. Baena, and R. Prasad, "Medium access techniques in ultra-wideband ad hoc networks," in *Proc. 6th National Conf. of Society for Electronic, Telecommun., Automatics, and Informatics (ETAI)*, Ohrid, Macedonia, Sep. 2003.
- [17] F. Cuomo, C. Martello, A. Baiocchi, and F. Capriotti, "Radio resource sharing for ad hoc networking with UWB," *IEEE J. Select. Areas Commun.*, vol. 20, no. 9, pp. 1722–1732, Dec. 2002.
- [18] H. Zu and A. Ganz, "A radio resource control method in UWB MAC protocol design," in *Proc. IEEE Military Commun. Conf. (MILCOM)*, vol. 2, Boston, MA, Oct. 2003, pp. 886–891.
- [19] E. Fishler and H. V. Poor, "On the tradeoff between two types of processing gain," in *Proc. 40th Annual Allerton Conf. on Commun. Control Computing*, Monticello, IL, Oct. 2002.

- [20] W. R. Heinzelman, A. Chandrakasan, and H. Balakrishnan, "Energy efficient communication protocol for wireless microsensor networks," in *Proc. Annual Hawaii International Conference on System Sciences*, Hawaii, Jan. 2000, pp. 3005–3013.
- [21] "Federal Communications Commission: Revision of part 15 of the commission's rules regarding ultra-wideband transmission system," First Report and Order, ET Docket 98-153, FCC 02-48, April 2002.
- [22] S. Gezici, H. Kobayashi, H. V. Poor, and A. F. Molisch, "Performance evaluation of impulse radio UWB systems with pulse-based polarity randomization," *IEEE Trans. Sig. Processing*, vol. 53, no. 7, pp. 1–13, July 2005.
- [23] N. He and C. Tepedelenlioglu, "Adaptive synchronization for non-coherent uwb receivers," in *Proc. IEEE International Conference on Acoustics, Speech, and Signal Processing (ICASSP'04)*, vol. 4, Montreal, Quebec, Canada, May 2004, pp. 517–520.
- [24] S. Kullback, *Information theory and statistics*. Wiley, New York, 1959.
- [25] P. Billingsley, *Probability and Measure*. John Wiley & Sons, New York, 2nd edition, 1986.

APPENDIX

A. Proof of Lemma 1

From (2) and (3), the MAI from user k , M_k in (5), can be expressed as follows

$$M_k = \sqrt{\frac{E_{rp}^{(k)}}{N_s^{(\xi)}}} \sum_{l=0}^{N_s^{(\xi)}-1} M_{k,l}, \quad (27)$$

where

$$M_{k,l} = a_l^{(\xi)} \sum_{j=-\infty}^{\infty} a_j^{(k)} b_{\lfloor j/N_s^{(k)} \rfloor}^{(k)} R(jT_f^{(k)} - lT_f^{(\xi)} + c_j^{(k)}T_c - c_l^{(\xi)}T_c - \Delta_k T_c), \quad (28)$$

with $\Delta_k = (\tau_k - \tau_\xi)/T_c$ being the amount of asynchronism between the desired user and user k in terms of the chip interval, and $R(x) = \int_{-\infty}^{\infty} w_{rx}(t+x)w_{rx}(t)dt$.

First, consider the case in which $N_s^{(\xi)} \leq N_s^{(k)}$. It can be shown that $\{M_{k,l}\}_{l=0}^{N_s^{(\xi)}-1}$ form a 1-dependent sequence [25], which means that M_{k,l_1} and M_{k,l_2} are independent for $|l_1 - l_2| > 1$. This is due to the facts that the interference to frame l_1 and l_2 of the desired user always comes from different frames of user k for $|l_1 - l_2| > 1$, and that the random polarity codes are independent and identically distributed as binary random variables $(-1, +1)$. The random polarity codes also result in a zero mean distribution for each term of the sequence $\{M_{k,l}\}_{l=0}^{N_s^{(\xi)}-1}$; i.e., $E\{M_{k,l}\} = 0$ for $l = 0, 1, \dots, N_s^{(\xi)} - 1$.

For a 1-dependent zero mean sequence, the central limit theorem for dependent sequences can be applied to obtain the asymptotic distribution of $\frac{1}{\sqrt{N_s^{(\xi)}}} \sum_{l=0}^{N_s^{(\xi)}-1} M_{k,l}$, as $N_s^{(\xi)} \rightarrow \infty$, as $\mathcal{N}\left(0, E\{M_{k,l}^2\} + 2E\{M_{k,l}M_{k,l+1}\}\right)$ [25].

It can be shown that the correlation terms are zero due to the fact that random polarity codes are zero mean and independent for different indices. Also after some manipulation, it can be shown that $E\{M_{k,l}^2\} = 1/N_h^{(k)}$. Hence, it is obtained that

$$\sqrt{\frac{E_{rp}^{(k)}}{N_s^{(\xi)}}} \sum_{l=0}^{N_s^{(\xi)}-1} M_{k,l} \sim \mathcal{N}\left(0, \frac{E_{rp}^{(k)}}{N_h^{(k)}}\right), \quad (29)$$

as $N_s^{(\xi)} \rightarrow \infty$. Therefore, for large $N_s^{(\xi)}$, M_k in (27) can be approximated as in (9).

For $N_s^{(\xi)} > N_s^{(k)}$, the MAI from user k can be expressed as the summation of frame interference terms as

follows:

$$M_k = \sqrt{\frac{E_{rp}^{(k)}}{N_s^{(\xi)}}} \sum_{l=0}^{N_s^{(k)}} \hat{M}_{k,l}, \quad (30)$$

where $\hat{M}_{k,l}$ is the interference related to the l th frame of user k :

$$\hat{M}_{k,l} = a_l^{(k)} b_{\lfloor l/N_s^{(k)} \rfloor}^{(k)} \sum_{j=0}^{N_s^{(\xi)}-1} a_j^{(\xi)} R(jT_f^{(k)} - lT_f^{(\xi)} + c_j^{(k)}T_c - c_l^{(\xi)}T_c - \Delta_k T_c). \quad (31)$$

It can be shown that $\{\hat{M}_{k,l}\}_{l=1}^{N_s^{(k)}-1}$ form a 1-dependent sequence³. Then, as $N_s^{(k)} \rightarrow \infty$,

$$\frac{1}{\sqrt{N_s^{(k)}}} \sum_{l=1}^{N_s^{(k)}-1} \hat{M}_{k,l} \sim \mathcal{N}\left(0, \frac{1}{N_h^{(\xi)}}\right). \quad (32)$$

For large $N_s^{(k)}$, M_k is approximately distributed as $\mathcal{N}\left(0, E_{rp}^{(k)} \frac{N_s^{(k)}}{N_s^{(\xi)} N_h^{(\xi)}}\right)$. However, since the total gain N_c is constant for all users; that is, $N_s^{(k)} N_h^{(k)} = N_s^{(\xi)} N_h^{(\xi)}$, the variance is the same as that in (9).

All in all, for large values of $\min\{N_s^{(k)}, N_s^{(\xi)}\}$, the distribution of the MAI from user k is approximately given by (9). \square

B. Proof of Lemma 2

The proof is similar to the proof in Appendix A. First, consider the case in which $N_s^{(\xi)} < N_s^{(k)}$. The MAI from user k can be expressed, from (19)-(23), as

$$M_k = \sqrt{\frac{E_{rp}^{(k)}}{N_s^{(\xi)}}} \sum_{j=0}^{N_s^{(\xi)}-1} M_{k,j}, \quad (33)$$

where

$$M_{k,j} = a_j^{(1)} \sum_{m=-\infty}^{\infty} a_m^{(k)} b_{\lfloor m/N_s^{(k)} \rfloor}^{(k)} \phi_{uv}^{(k)}\left(mT_f^{(k)} - jT_f^{(1)} + (c_m^{(k)} - c_j^{(1)})T_c + \Delta_k T_c\right), \quad (34)$$

with $\phi_{uv}^{(k)}(x)$ being defined as

$$\phi_{uv}^{(k)}(x) = \int_{-\infty}^{\infty} u^{(k)}(t-x)v(t)dt. \quad (35)$$

Note that $\{M_{k,j}\}_{j=0}^{N_s^{(\xi)}}$ forms a 1-dependent sequence [25] since it is assumed that the delay spreads of the channels are smaller than the frame intervals, which results in different interference terms for each pair of interference terms M_{k,j_1} and M_{k,j_2} for $|j_1 - j_2| > 1$.

Due to the distribution of the polarity codes, the mean and correlation terms can be shown to be zero; i.e., $E\{M_{k,j}|\Delta_k\} = 0$, and $E\{M_{k,j}M_{k,l}|\Delta_k\} = 0$ for $l \neq j$. In order to calculate the variance, the facts that the polarity

³As $N_s^{(k)} \rightarrow \infty$, the edge values, $\hat{M}_{k,0}$ and $\hat{M}_{k,N_s^{(k)}}$ can be omitted for simplicity.

codes are independent for different user and frame indices, and that the TH sequences are uniformly distributed are employed. Then, it can be shown that

$$\mathbb{E}\{M_{k,j}^2|\Delta_k\} = \frac{1}{N_h^{(\xi)} N_h^{(k)}} \sum_{i=0}^{N_h^{(k)}-1} \sum_{l=0}^{N_h^{(\xi)}-1} \sum_{m=-\infty}^{\infty} \left\{ \phi_{uv}^{(k)} \left(mT_f^{(k)} - jT_f^{(\xi)} + (i-l)T_c + \Delta_k T_c \right) \right\}^2, \quad (36)$$

which reduces, after some manipulation, to

$$\mathbb{E}\{M_{k,j}^2|\Delta_k\} = \frac{1}{N_h^{(k)}} \sum_{j=-(L-1)}^{L-1} \left[\phi_{uv}^{(k)}(jT_c) \right]^2. \quad (37)$$

From (35), (20) and (22), (37) can be expressed as

$$\mathbb{E}\{M_{k,j}^2|\Delta_k\} = \frac{1}{N_h^{(k)}} \left[\sum_{j=1}^L \left(\sum_{i=1}^j \beta_i \alpha_{i-j+L}^{(k)} \right)^2 + \sum_{j=1}^{L-1} \left(\sum_{i=1}^j \alpha_i^{(k)} \beta_{i-j+L} \right)^2 \right]. \quad (38)$$

Note that the result is independent of the offset Δ_k . Therefore, $\mathbb{E}\{M_{k,j}^2\}$ is given by (38), as well.

Since $\{M_{k,j}\}_{j=0}^{N_s^{(\xi)}-1}$ is a 1-dependent sequence with zero mean and correlation terms, the distribution of $\sqrt{\frac{E_{rp}^{(k)}}{N_s^{(\xi)}} \sum_{j=0}^{N_s^{(\xi)}-1} M_{k,j}}$ converges to the Gaussian distribution given by $\mathcal{N}\left(0, E_{rp}^{(k)} \mathbb{E}\{M_{k,j}^2\}\right)$, as $N_s^{(\xi)} \rightarrow \infty$ [25]. Then, (24) follows from (38) for the $N_s^{(\xi)} < N_s^{(k)}$ case.

For $N_s^{(\xi)} \geq N_s^{(k)}$, the MAI from user k can be expressed as $M_k = \sqrt{\frac{E_{rp}^{(k)}}{N_s^{(\xi)}} \sum_{j=0}^{N_s^{(k)}} \hat{M}_{k,j}}$, where $\hat{M}_{k,j}$ denotes the interference related to the j th frame of user k . Then, by similar arguments, (24) can be derived.

Therefore, the result in Lemma 2 is obtained as $\min\{N_s^{(\xi)}, N_s^{(k)}\} \rightarrow \infty$.

□

List of Table and Figure Captions:

Fig. 1: The received signals from multiple users and the correlator receiver.

Fig. 2: Example transmitted signals for a) Fixed frame duration, and b) Fixed throughput.

Fig. 3: KL distances for case 2 with respect to $N_s^{(\xi)}$ and $N_h^{(k)}$. Only two users with equal power are considered.

Fig. 4: Comparison of theoretical and simulation BERs for *case 1*. Only two users with equal power are considered ($N_h = 10$).

Fig. 5: Remaining aggregate energy in the network with respect to time.

Fig. 6: Number of alive nodes in the network with respect to time.

Fig. 7: The ratio of the time periods for the proposed and conventional techniques where the total network energy falls to 95% of the initial network energy.

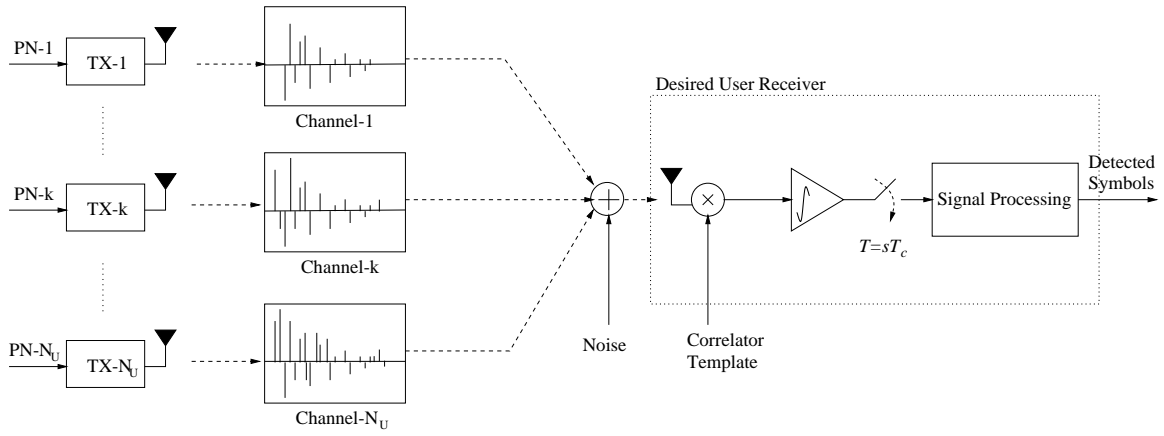


Fig. 1.

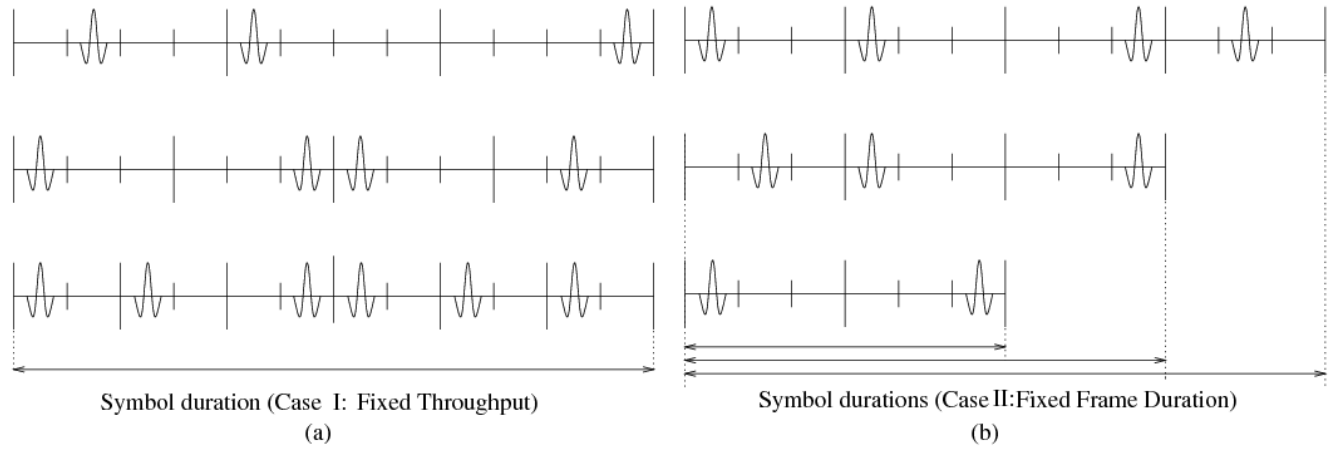


Fig. 2.

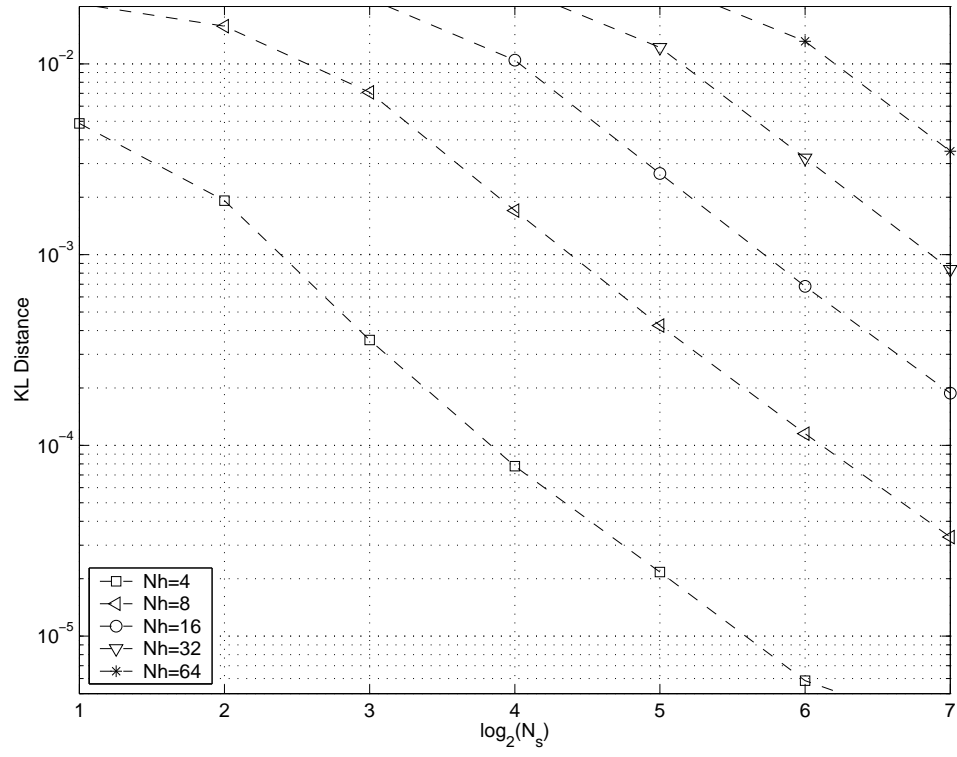


Fig. 3.

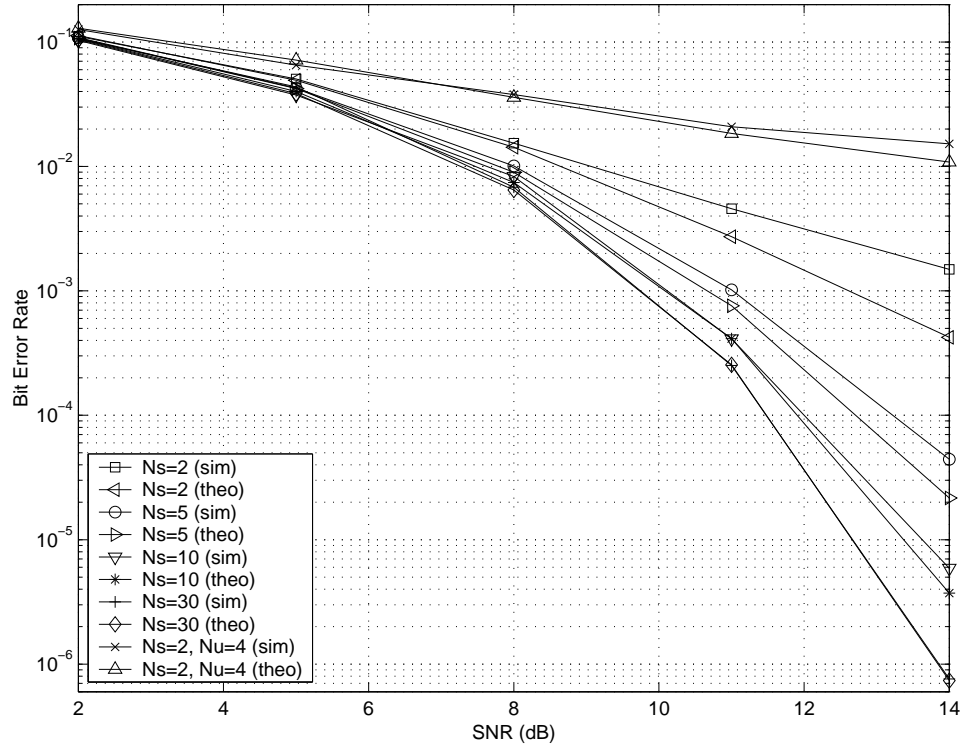


Fig. 4.

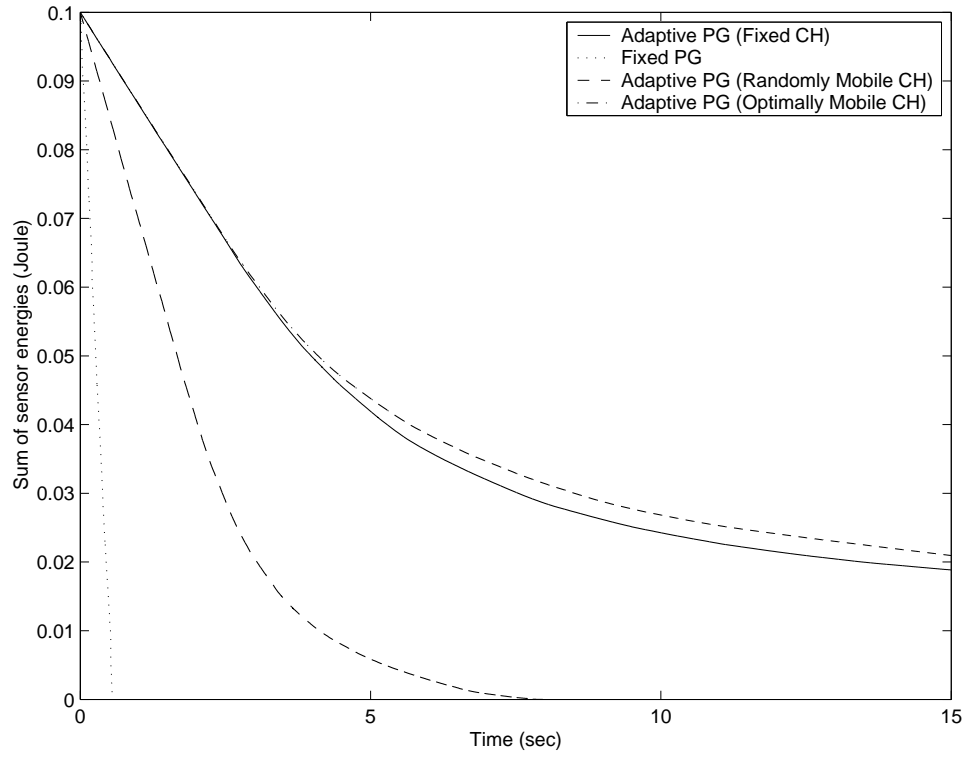


Fig. 5.

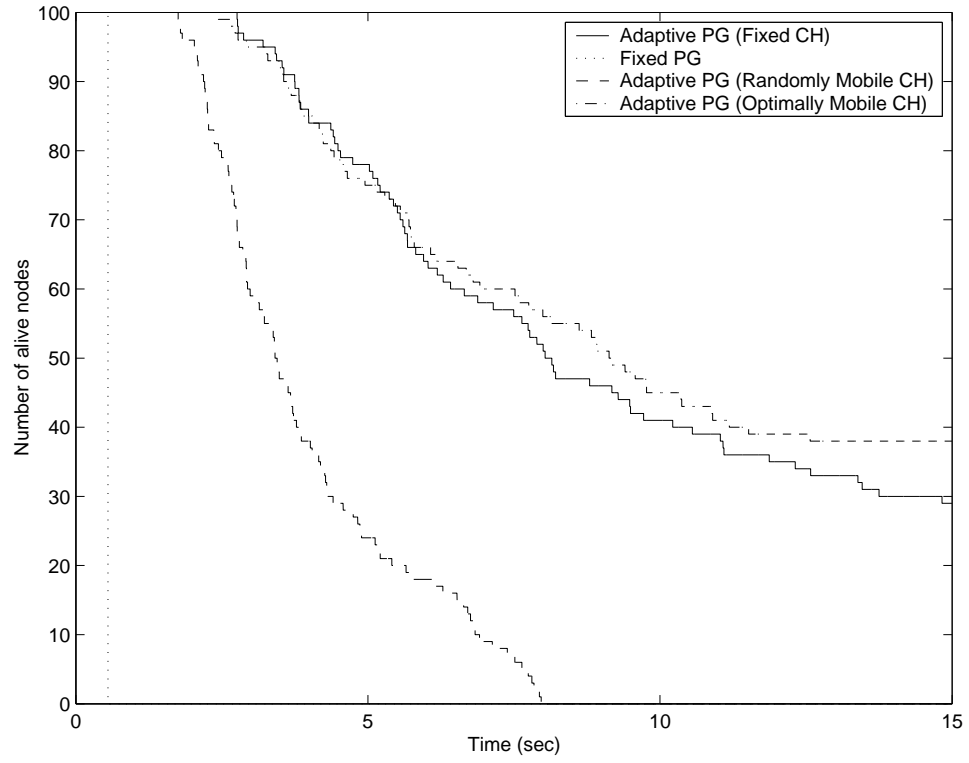


Fig. 6.

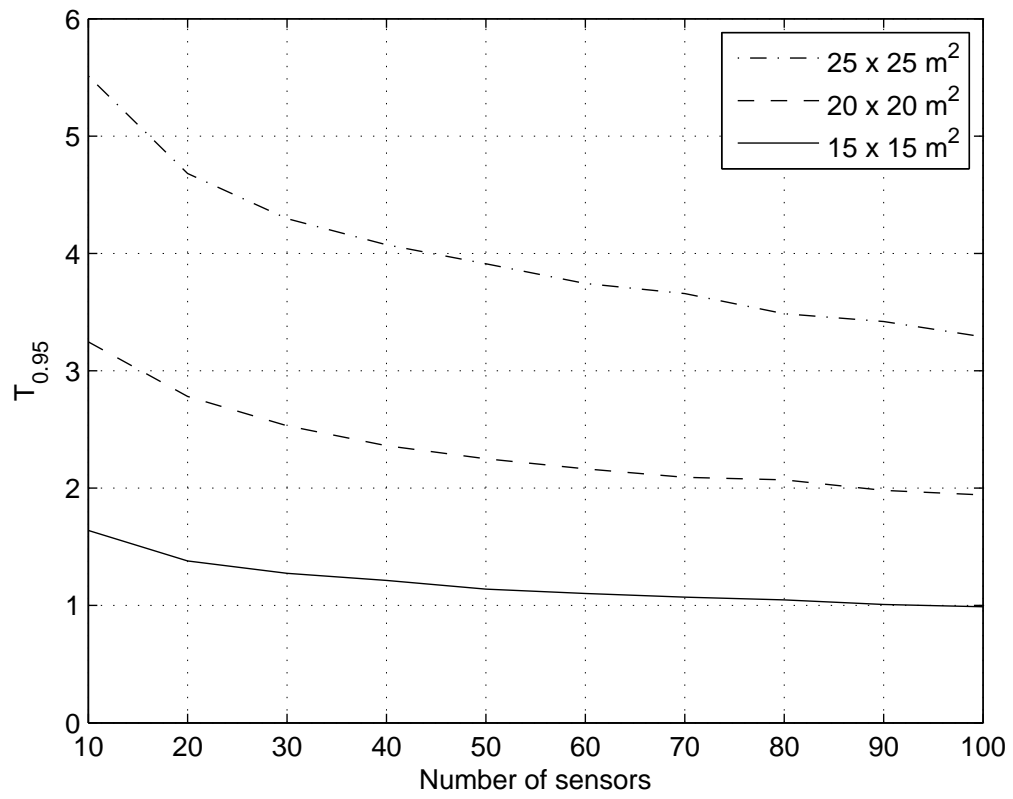


Fig. 7.